Carbohydrate Polymers 111 (2014) 366–373

Contents lists available at ScienceDirect

Carbohydrate Polymers

journal homepage: www.elsevier.com/locate/carbpol

Thermoresponsive chitosan–agarose hydrogel for skin regeneration

Sónia P. Miguel[a], Maximiano P. Ribeiro[a,b], Hugo Brancal[a], Paula Coutinho[a,b], Ilídio J. Correia[a,*]

[a] CICS-UBI, Health Sciences Research Centre, Faculty of Health Sciences, University of Beira Interior, 6200-506 Covilhã, Portugal
[b] UDI-IPG, Research Unit for Inland Development, Polytechnic Institute of Guarda, Guarda, Portugal

ARTICLE INFO

Article history:
Received 29 January 2014
Received in revised form 24 April 2014
Accepted 27 April 2014
Available online 2 May 2014

Keywords:
Antimicrobial activity
Biocompatibility
Hydrogel
Skin substitutes
Wound healing

ABSTRACT

Healing enhancement and pain control are critical issues on wound management. So far, different wound dressings have been developed. Among them, hydrogels are the most applied.

Herein, a thermoresponsive hydrogel was produced using chitosan (deacetylation degree 95%) and agarose. Hydrogel bactericidal activity, biocompatibility, morphology, porosity and wettability were characterized by confocal microscopy, MTS assay and SEM. The performance of the hydrogel in the wound healing process was evaluated through *in vivo* assays, during 21 days.

The attained results revealed that hydrogel has a pore size (90–400 μm) compatible with cellular internalization and proliferation. A bactericidal activity was observed for hydrogels containing more than 188 μg/mL of chitosan. The improved healing and the lack of a reactive or a granulomatous inflammatory reaction in skin lesions treated with hydrogel demonstrate its suitability to be used in a near future as a wound dressing.

1. Introduction

Burned patients may experience a wide number of potentially fatal complications including shock, infection, electrolyte imbalances and respiratory failure (Böttcher-Haberzeth, Biedermann, & Reichmann, 2010). Furthermore, they can also experience severe psychological and emotional distress due to long periods of hospitalization, scarring and deformity (Evers, Bhavsar, & Mailänder, 2010). Such, highlights the importance of developing new wound dressings that improve the healing process, making it less painful and, simultaneously, contribute for the reestablishment of skin structure and functions in a shorter period of time (Atiyeh & Hayek, 2005; Metcalfe & Ferguson, 2007).

Among the different wound dressers produced so far, hydrogels due to their intrinsic properties are the ones that better mimic the extracellular matrix (ECM) and have the potential to direct cell migration, adhesion and growth during tissue regeneration, events that are crucial for skin regeneration (Lakes, 2007; Nicodemus & Bryant, 2008; Yu & Ding, 2008). When applied at the wound site hydrogels promote a moist healing and cool the surface of the wound, which may lead to a relevant reduction in pain and therefore have high patient acceptability (Balakrishnan, Mohanty, Umashankar, & Jayakrishnan, 2005; Boateng, Matthews, Stevens, & Eccleston, 2008). Some hydrogels have the particularity of gelling within the desired tissue or body cavity as a result of polymer interactions. Such *in situ*-forming systems advantageously flow freely as injectable liquids before administration and gel under physiological conditions. Temperature-sensitive systems that gel at body temperature are especially attractive (Schuetz, Gurny, & Jordan, 2008).

Herein, the main goal of this study was to produce a new *in situ* thermoresponsive hydrogel composed by agarose and chitosan to be used as an injectable scaffold for tissue regeneration. As described above *in situ* formed hydrogels are mouldable, *i.e.*, are able to acquire the right shape at the wound site, without wrinkling or fluting and interacting with the damaged tissue.

Agarose is a biocompatible linear polysaccharide extracted from marine algae (Buckley, Thorpe, O'Brien, Robinson, & Kelly, 2009), consisting of 1,4-linked 3,6-anhydro-α-L-galactose and 1,3-linked β-D-galactose derivatives that forms thermorreversible gels with suitable properties for tissue engineering applications (Xu et al., 2005). The mechanical properties presented by agarose are similar to those of tissues and can be easily tailored by varying polymer concentration. When solubilized in water, it forms a gel with a rigid network, resulting on a three-dimensional porous structure providing a good environment for cell adhesion, spreading and proliferation (Cao, Gilbert, & He, 2009; Mano et al., 2007; Martin,

* Corresponding author. Tel.: +351 275 329 002/+351 275 329 003; fax: +351 275 329 099.
E-mail address: icorreia@ubi.pt (I.J. Correia).

http://dx.doi.org/10.1016/j.carbpol.2014.04.093
0144-8617/

Minner, Wiseman, Klank, & Gilbert, 2008; Trivedi, Rao, & Kumar, 2014).

Furthermore, agarose hydrogels may be polymerized *in situ* reducing invasiveness of the surgery and also allow the hydrogel to acquire the required shape (Varoni et al., 2012).

Chitosan, the partially acetylated cationic (1–4)-2-amino-2-deoxy-β-D-glucan, is industrially produced from marine chitin. Its regenerative properties have been amply recognized (Busilacchi, Gigante, Mattioli-Belmonte, Manzotti, & Muzzarelli, 2013). In acidic aqueous solutions the protonated free amino groups of glucosamine promote the solubility of this polymer. Its hydrophilic surface promotes cell adhesion, proliferation and differentiation (Francis Suh & Matthew, 2000; Hutmacher, Goh, & Teoh, 2001; Muzzarelli, 2009). Chitosan derivatization allows an extensive adjustment of mechanical and biological properties, contributing for its anticholesterolemic and antimicrobial activity, biocompatibility, biodegradability, hemostasis and capacity to stimulate the healing process (Felt, Carrel, Baehni, Buri, & Gurny, 2000; Hirano & Noishiki, 2004; Li, Ramay, Hauch, Xiao, & Zhang, 2005; Muzzarelli, 1997).

The interaction of chitosan and agarose allows the production of hydrogels capable of gelling within the desired site, as a result of polymer interactions.

In this study, deacetylated chitosan was combined with agarose in order to explore the polymeric interactions and the thermosensitive character of agarose for producing a hydrogel. The produced hydrogel was characterized through *in vitro* and *in vivo* assays, in order to evaluate its suitability for being used as a wound dressing.

2. Materials and methods

2.1. Materials

Agarose (low melting point-ultrapure grade) was acquired from Nzytech (Lisboa, Portugal). Amphotericin B, Bovine serum albumin (BSA), Chitosan (medium molecular weight (MMW) (degree of deacetylation: 83.35% ± 0.23); Dulbecco's modified Eagle's medium (DMEM-F12), Ethylenediaminetetraacetic acid (EDTA), LB Broth, Kanamycin, *N*-acetyl-D-glucosamine, phosphate-buffered saline solution (PBS), resazurin (7-hydroxy-3*H*-phenoxazin-3-one-10-oxide), streptomycin and trypsin were purchased from Sigma-Aldrich (Sintra, Portugal). Acetic acid and sodium hydroxide were bought to Pronalab (Barcelona, Spain). Normal human dermal fibroblasts adult (NHDF), criopreserved cells were purchased from PromoCell (Labclinics, S.A.; Barcelona, Spain). *Staphylococcus aureus* (*S. aureus*) ATCC 25923 was used to evaluate antimicrobial properties of hydrogel. Fetal bovine serum (FBS) (free from any antibiotic and heat inactivated) was acquired from Biochrom AG (Berlin, Germany). 3-(4,5-dimethylthiazol-2-yl)-5-(3-carboxymethoxyphenyl)-2-(4-sulfophenyl)-2*H*-tetrazolium (MTS) was purchased from Promega (Canada, USA). Tris Base was obtained from Fisher Scientific (Portugal).

2.2. Synthesis and characterization of deacetylated chitosan

Chitosan was deacetylated by adapting a method previously described in literature (Gaspar, Sousa, Queiroz, & Correia, 2010) and then purified. The recovered chitosan was dissolved in 1 M acetic acid solution filtered with a 0.22 μm filter to remove traces of any solid particles. Afterwards, the pH was adjusted to 7 with 1 M NaOH, which resulted in the precipitation of the chitosan material. The product was then centrifuged at 4500 rpm (Sigma 3K18C centrifuge), this procedure was repeated three times and finally the recovered pellet was lyophilized for one day. The degree of deacetylation was measured by using the first derivative UV-spectroscopy (1DUVS) method (Muzzarelli & Rocchetti, 1985). UV–vis chitosan spectra were obtained using a Shimadzu 1700 UV–vis spectrophotometer. Table S1 shows the degree of deacetylation for the commercial and deacetylated chitosan samples. The chitosan used for hydrogel production had a deacetylation degree of 95.08% ± 0.48, meaning that almost all of the primary amine groups of the chitosan polymer chain are positively charged.

2.3. Production of chitosan–agarose hydrogel

For chitosan–agarose hydrogel (CAH) production, different percentages of deacetylated chitosan (from 0.75% to 2.5%), previously filtered with a 0.22 μm filter, were initially dissolved in 1% acetic acid solution. Then, agarose powder was added to the chitosan solution, under stirring at 50 °C, until reaching a final concentration of 3%, w/v (please see Table S2 for further details).

2.4. Determination of contact angle of CAH

Contact angles of CAH (3% agarose–0.75% chitosan and 3% agarose–1.5% chitosan) were determined using a data physics contact angle system OCAH 200 apparatus, operating in static mode. For each sample, water drops were placed at various locations of the materials surface, at room temperature (RT). The reported contact angles are the average of at least three measurements.

2.5. Study of water uptake ability (swelling)

To evaluate CAH (3% agarose–1.5% chitosan) water uptake ability, a known weight (W_0) of the hydrogel was immersed in 1 mL Tris buffer, at pH 5 and 37 °C ($n = 5$). At predetermined intervals the swollen CAH was removed from the solution, the excess of water removed with filter paper, and subsequently weighted (W_t) (Zhang, Guo, Peng, & Jin, 2004). The swelling ratio was evaluated by using Eq. (1):

$$\text{swelling ratio } (\%) = \frac{W_t - W_0}{W_0} \times 100$$

where W_t is the final weight and W_0 is the initial weight of CAH.

2.6. Proliferation of human fibroblast cells in the presence of CAH

To evaluate NHDF growth in the presence of CAH, cells were seeded in 96-well plates, containing the hydrogel, at a density of 2×10^4 cells/cm^2 per well, and incubated at 37 °C in a 5% CO_2 humidified atmosphere, for 24 and 72 h. Cell growth was monitored by using an Olympus CX41 inverted light microscope (Tokyo, Japan) equipped with an Olympus SP-500 UZ digital camera.

2.7. Characterization of the cytotoxic profile of CAH

To evaluate NHDF cell viability in the presence of CAH an MTS assay was used. First, 2×10^4 cells per well were seeded on CAH surface. After 24 and 72 h of incubation at 37 °C, the culture medium was removed and replaced by a mixture of 100 μL of fresh culture medium and 20 μL of MTS/PMS (phenazine methosulfate) reagent solution. Then, cells were incubated for 4 h, at 37 °C, under a 5% CO_2 humidified atmosphere. Subsequently the absorbance was measured at 492 nm using a microplate reader (Sanofi, Diagnostics Pauster). Ethanol 96% was added to cells to be used as positive controls (K^+), whereas cells without biomaterials were used as negative controls (K^-) (Bhat & Kumar, 2012; Marques, Gaspar, Costa, Paquete, & Correia, 2014; Palmeira-de-Oliveira et al., 2010; Ribeiro et al., 2009).

2.8. Scanning electron microscopy analysis

CAH (3% agarose–0.75% chitosan and 3% agarose–1.5% chitosan) morphology with/without adhered NHDF cells was characterized by scanning electron microscopy (SEM), using a procedure previously described elsewhere (Ribeiro et al., 2009). Briefly, samples were dehydrated in graded ethanol (ETOH) of 70, 80, 90, and 100%, 5 min each. Then, hydrogels were mounted on an aluminium board using a double-sided adhesive tape and sputter coated with gold using an Emitech K550 (London, England) sputter coater. A Hitachi S-2700 (Tokyo, Japan) scanning electron microscope operated at an accelerating voltage of 20 kV and at various magnifications (Ribeiro et al., 2009) was used for samples analysis.

2.9. Confocal microscopy analysis

For the visualization of NHDF cells within CAH (3% agarose–1.5% chitosan), 10×10^3 cells/mL were seeded in μ-Slide 8 well Ibidi imaging plates (Ibidi GmbH, Germany) in contact with hydrogel. After 24 h, cells were fixed with 4% paraformaldehyde (PFA) in PBS for 20 min and then stained with 1 μL of Propidium Iodide (PI) (1 mg/mL) during 15 min, at 37 °C. Imaging experiments were performed in a Zeiss LSM 710 laser scanning confocal microscope (CLSM) (Carl Zeiss SMT Inc., USA), where consecutive z-stacks were acquired. 3D reconstruction and image analysis was performed in Zeiss Zen 2010 (Gaspar et al., 2011; Lima et al., 2013).

2.10. Characterization of the antibacterial properties of CAH

2.10.1. Determination of minimum inhibitory concentration of CAH

S. aureus, a Gram-positive bacteria, was used to evaluate the antimicrobial properties of CAH. *S. aureus* (1×10^6 colony-forming units (CFU)/mL) was inoculated in culture medium (LB Broth). Then, several formulations of CAH with 3% agarose and different concentrations of Chitosan (125–400 μg/mL) were tested. A negative (without CAH) and a positive control (containing Kanamycin antibiotic (30 mg/mL)) were also prepared. Then, the 96-well plate was incubated for 24 h, at 37 °C. For monitoring bacterial growth, 10 μL of resazurin (0.1%) was added and, after 24 h, the fluorescence was measured using a fluorescence plate reader with filter set Ex545/Em590 (Aziz, Cabral, Brooks, Moratti, & Hanton, 2012).

2.10.2. Evaluation of biofilm deposition at CAH surface

S. aureus proliferation at CAH surface was also evaluated by SEM analysis (Correia et al., 2013). Defined concentrations of CAH were placed on the surface of a plate of LB agar, in contact with *S. aureus* (1×10^8 CFU/mL), without any other antimicrobial agent. Then the petri plate was incubated for 24 h, at 37 °C. After, the morphologies of CAH with/without *S. aureus* were analyzed by acquiring SEM images.

2.11. In vivo assays

To perform the *in vivo* assays, a total of 10 Wistar rats (8–10 weeks) weighing between 150 and 200 g were used. The animal protocols followed in the present study were performed according to the guidelines set forth in the National Institutes of Health Guide for the care and use of laboratory animals. The experimental setup was performed according to that previously used by Ribeiro et al. (2009). Animals were separated into two groups: in group 1, wounds were filled with CAH (3% agarose–1.5% chitosan); whereas in the second group, used as control, wounds were covered with serum physiologic solution. During the study, animals were kept in separate cages and were fed with commercial rat food and water *ad libitum*.

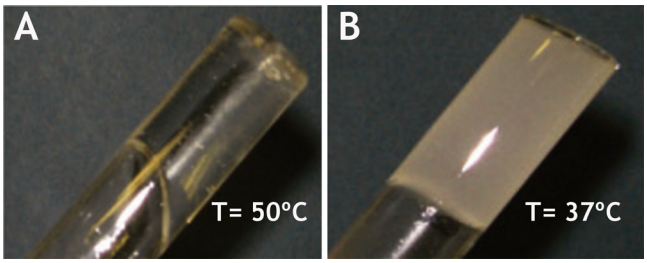

Fig. 1. Macroscopic images of CAH at 50 °C (A) and 37 °C (B).

To follow the wound healing process, animals were photographed with a digital camera (NikonD50) along time. Then the wound size (WS) was determined by using an image analysis software ImageJ (Scion Corp., Frederick, MD). Animals were sacrificed after 7, 14 and 21 days.

2.12. Histological analysis

To evaluate the local and systemic immune response of the host to CAH, tissue specimens were obtained from each wound area by sharp dissection at days 7, 14 and 21. The samples of skin tissues were obtained by necropsy, formalin fixed and paraffin embedded for routine histological processing. A 3 μm section was obtained from each sample using a cryostat microtome (Leica CM1900) and then stained with hematoxylin and eosin (H&E). Subsequently, samples were observed using a light microscope with a specific image analysis software from Zeiss. Skin fragments with no hydrogel were used as control. Brain, lung, liver, spleen and kidney samples, obtained by necropsy, were also analysed to check for any morphological alteration (Ribeiro, Morgado, Miguel, Coutinho, & Correia, 2013; Ribeiro et al., 2009).

3. Results and discussion

3.1. Characterization of the morphology of CAH

The CAH produced in this study gels when the temperature decreases from 50 °C to 37 °C, changing from transparent to opaque (see Fig. 1). The thermoresponsive character of CAH is attributed to agarose, that undergoes through a reversible gelling process without losing its mechanical and thermal properties (Medina-Esquivel, Freile-Pelegrin, Quintana-Owen, Yáñez-Limón, & Alvarado-Gil, 2008). In the literature it is described that at high temperatures polymeric chains have a random coil conformation. By lowering temperature they start to form double helices and aggregates that act as physical junctions of the gels (Jeong, Kim, & Bae, 2012).

When tissue engineering applications are envisioned, cell adhesion to biomaterials is a crucial prerequisite to allow tissue regeneration (Faucheux, Schweiss, Lützow, Werner, & Groth, 2004). Among the different factors affecting cell adhesion, materials surface charge, morphology and porosity are considered the most relevant.

SEM images presented in Fig. 2 show that CAH has an irregular surface and a porous interconnected structure, with pore diameters (90–400 μm), that allow a good cell penetration and proliferation in contact with hydrogel, as well as nutrients and oxygen diffusion into the bulk of the matrix (Kathuria, Tripathi, Kar, & Kumar, 2009; Silva et al., 2013).

3.1.1. Contact angle of CAH

To evaluate the hydrophilic character of CAH surface water contact angles were determined. The CAH, 3% agarose–0.75%

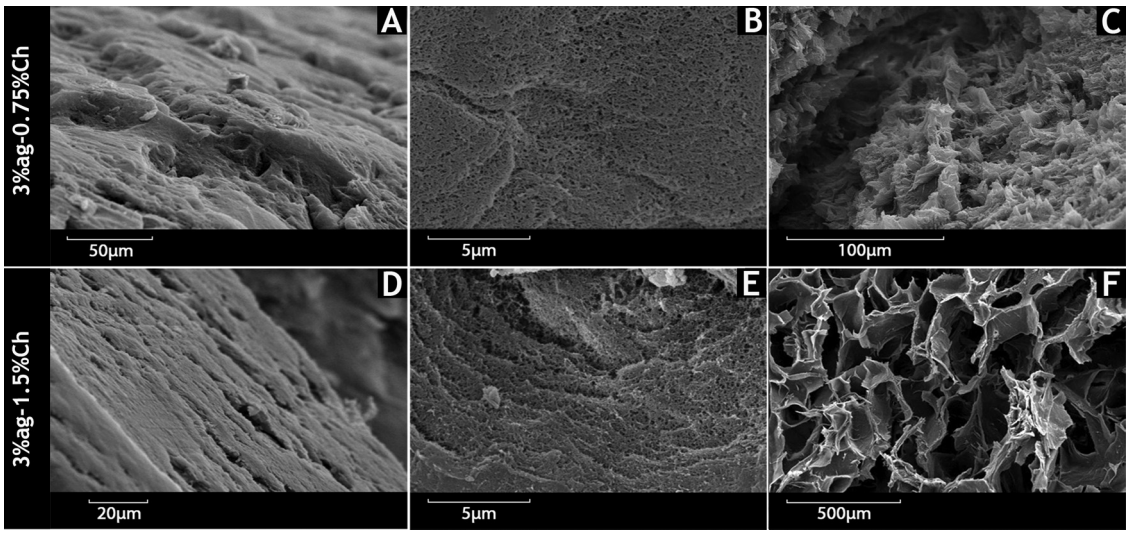

Fig. 2. SEM images of CAH: cross section of CAH (3% ag–0.75% Ch) (A); surface of CAH (3% ag–0.75%Ch) (B); inner structure of CAH (3% ag–0.75% Ch) (C); cross section of the CAH of CAH (3% ag–1.5% Ch) (D); surface of CAH (3% ag–1.5% Ch) (E); inner porous network of CAH (3% ag–1.5% Ch) (F).

chitosan and 3% agarose–1.5% chitosan, presented contact angles of 40.9° ± 3.8° and 43.7° ± 3.7°, respectively. Such values demonstrate the moderate hydrophilic character of the hydrogels produced. According to what was previously described in literature, the surface is considered hydrophobic when the contact angle is between 90° and 150°and hydrophilic when it is comprehended 10° and 90°. Cell adhesion to materials occurs in optimal conditions when the polymer surfaces present a moderate wettability, with water contact angles ranging 40–70° (Oliveira, Alves, & Mano, 2012).

3.1.2. Study of water uptake ability of CAH

To evaluate the appropriateness of CAH for this biomedical application, its swelling behavior was studied (Fig. S1). The obtained results demonstrated that the high water uptake capacity of CAH after 12 h, caused an increase in the pore diameter of the polymeric mesh and subsequent diffusion of nutrients, cells, bioactive molecules and waste along hydrogel (Valente, Gaspar, Antunes, Countinho, & Correia, 2012). Such swelling behavior can be explained by the presence of hydrophilic groups, such as hydroxyl, amino and carboxyl groups that can be easily hydrated, both in chitosan and agarose (Bhat, Tripathi, & Kumar, 2011; Pasparakis & Bouropoulos, 2006).

3.2. Evaluation of cell viability and proliferation in the presence of CAH

In vitro studies were performed using fibroblasts as model cells, since they are essential for the of wound healing process to occur. These cells are involved in collagen, fibronectin, and synthesis of other biomolecules, that are structural components of the ECM, that provide a 3D support for the closure of tissue gaps and allow the restoration of the mechanical strength of the skin (Reinke & Sorg, 2012).

Fig. S2 shows that cells adhered and remained viable in contact with the hydrogel and in the negative control (K^-), where cell spreading and elongation was visualized. Such process is comprised of a cascade of four different partly overlapping events: cell attachment, cell spreading, organization of actin cytoskeleton, and formation of focal adhesions (Hersel, Dahmen, & Kessler, 2003). The cellular response or interaction with the 3D polymeric matrices is mediated by integrins that recognize specific motifs at materials surface and allow physical anchoring as well as in signal transduction mechanisms that occur at the cell membrane (Hersel et al., 2003; van der Flier & Sonnenberg, 2001). In the positive control (K^+), no cell adhesion or proliferation was observed. Dead cells with their typical spherical shape were observed.

To further characterize cell adhesion to materials surface a SEM analysis was also performed (see Fig. 3A). Fibroblasts attached and spread across the surface, presenting a round shape configuration, with some cytoplasm extensions toward the substrate after 24 h of being seeded on CAH surface. After 72 h, cells already presented the typical fibroblastic morphology, lamellipodia connecting to surrounding fibroblast were visualized and a continuous layer of cells started to be formed (Ribeiro et al., 2009). The cell behavior observed can be explained by the interaction of glycosaminoglycans, present at cell membrane, with the amine groups of chitosan present in CAH (Lee, Lim, Chong, & Shim, 2009; Ribeiro et al., 2009). Moreover, chitosan provides a matrix for 3D tissue growth and activates macrophages at the wound site that stimulate cell proliferation and histoarchitectural tissue organization (Jayakumar, Prabaharan, Sudheesh Kumar, Nair, & Tamura, 2011).

In addition, fibroblast cells migration and proliferation within CAH was also characterized by confocal microscopy analysis. The CLSM images presented in Fig. 3B show that cells were able to migrate to the inner structure of CAH and the hydrogel pores were sufficiently large (90–400 µm) to accommodate NHDF, after 24 h of culture, and also allow an effective nutrient supply and metabolic waste removal, processes that are essential for effective cell growth and subsequently skin regeneration (Kathuria et al., 2009; Weng, Romanov, Rooney, & Chen, 2008). Cellular internalization is further noticeable in the orthogonal projection shown in Fig. 3-b2.

3.3. Characterization of the cytotoxic profile of CAH

The materials cytocompatibility was also characterized through an MTS assay. The results presented in Fig. 3C show that the fibroblast cells viability was not affected, after 72 h of being in contact with CAH, highlighting the biocompatibility of the produced hydrogel. A statistically significant difference was noticed between the positive ($p < 0.01$) and the negative control and cells in contact with CAH. Moreover, the degradation by-products that could be produced during the 72 h did not affect cell viability, which is also important to allow the application of the hydrogel for the aimed biomedical application.

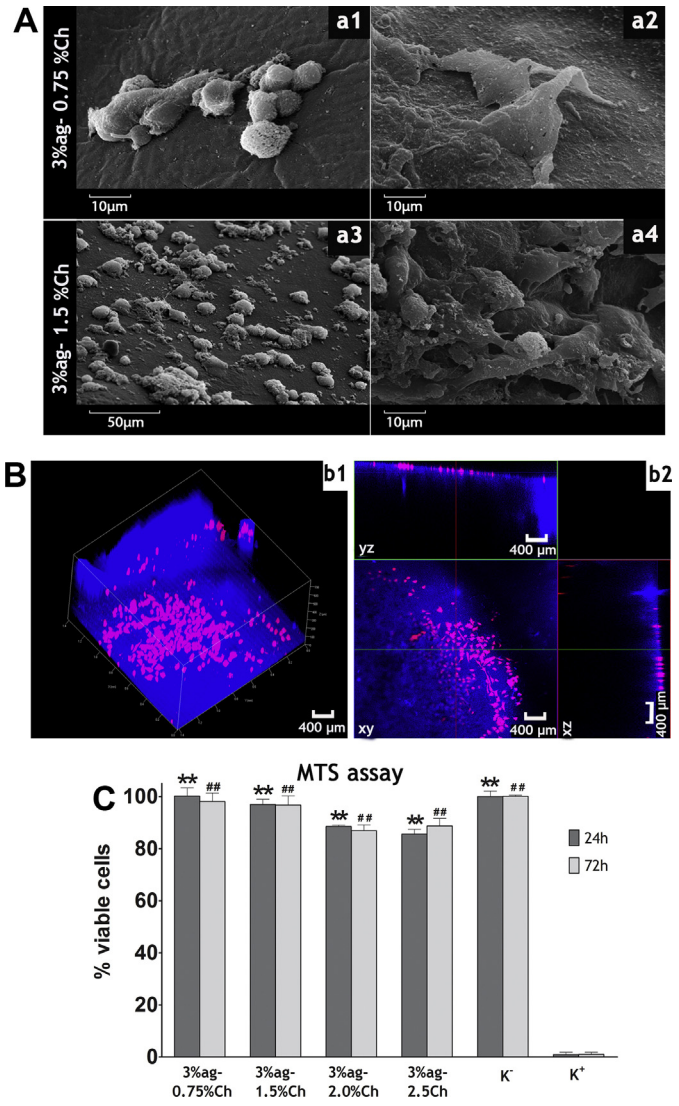

Fig. 3. Evaluation of cell behavior in contact with hydrogel: (A) SEM images of NHDF in contact with: CAH (0.75% Ch) after 24 h (a1) and 72 h (a2): CAH (1.5% Ch) after 24 h (a3) and 72 h (a4); (B) 3D reconstruction of the cell internalization in the CAH (1.5% Ch) using stacked CLSM images (b1); orthogonal projection of CAH (1.5% Ch) in *xy*, *yz* and *xz* plans (b2). (C) Evaluation of cell viability through an MTS assay after 24 and 72 h. K^+ (dead cells); K^- (live cells); Each result is the mean ± standart error of the mean of at least three independent experiments. Statistical analysis was performed using one-way ANOVA with Dunnet' post hoc test and Newman–Keuls multiple comparison test (**, $^{\#\#}$, $^{\#\#}$ $p < 0.01$).

3.4. Evaluation of the antimicrobial activity of the CAH

In this study, the CAH antibacterial properties were evaluated by standard tube dilution method using *S. aureus*. The bacterial strain was deemed appropriate for performing this assay, since it is reported in the literature as the most common gram-positive pathogen found in skin infections, when biomaterials are used for wound treatments (Juan, Zhimin, Anchun, Lei, & Jingchao, 2010).

Fig. 4A shows *S. aureus* incubated with several formulations of hydrogel, containing different concentrations of chitosan (ranging from 125 to 400 µg/mL), during 24 h at 37 °C. Afterwards, the CAH MIC values ranging between 188 and 200 µg/mL were determined (Fig. 4-a2) using a standard procedure, a resazurin assay, described in literature (Gonzalez & Tarloff, 2001). The results obtained revealed a significant difference between the test groups and the positive control ($p < 0.01$). CAH samples containing chitosan concentrations higher than 188 µg/mL exhibited antimicrobial activity, providing a defense barrier against the strain studied here. The polycationic chitosan, used in hydrogel production, can interact with the electronegative residues present at bacteria surface, increase the cell wall permeability and consequently the leakage of intracellular constituents and the dissipation of ionic gradients within bacteria (Kim et al., 2008; Mi et al., 2002).

The bacterial biofilm formation at the biomaterials surface is one of the main causes of implant rejection (Fedtke, Götz, & Peschel, 2004). These bacterial contaminations have the ability to evade host immune system response and also be resistant to different antibiotics (Fedtke et al., 2004). Biofilm formation at CAH surface was also evaluated through SEM analysis. *S. aureus* was added to different formulations of CAH, during 24 h as shown in Fig. 4 (b1–b2). The results attained revealed that biofilm formation only occurred in the negative control (Fig. 4-b3), where *S. aureus* was placed in agar plate without adding any antibacterial agent.

3.5. In vivo assays

The local and systemic histocompatibility of CAH was evaluated *in vivo*, by inducing transcutaneous full-thickness dermal wounds in Wistar rats. A minimum number of animals was used, taking into account the international guidelines set for animal experimentation. Wistar rats were initially divided into two groups. Group 1 was set as control, and wounds were only treated with serum physiologic solution. Group 2, test group, was used to study the influence of CAH (3% agarose–1.5% chitosan), that was chosen based on the results previously achieved *in vitro*, in the wound healing process. All animals showed good general health condition throughout the study, as assessed by their weight gain. CAH was applied directly at the wound site, at a temperature of 40 °C and gelled *in situ* at body temperature (37 °C). Fig. S3-A shows a set of typical wound beds after the surgical procedure and the different treatments to be applied (serum physiologic solution and CAH). The healing patterns were observed and wounds size measured for 21 days (Fig. S3-B). The wound size of animals from group 1 increased during the first days, while for the other group did not. Such result emphasizes the importance of an initial covering of the damage area with hydrogels, since they are usually composed by about 95% of water, gathering a moist environment that promotes wound re-epithelization by triggering epidermal cell migration at a speed of about 0.5 mm/day over a moist wound surface, which is twice as fast as that determined for dry wounds (Winter, 1974). Furthermore, chitosan possesses biological activities that affect macrophage function, stimulates cell proliferation and contributes for histoarchitectural tissue organisation, as already described elsewhere (Muzzarelli, 2009; Paul & Sharma, 2004). On the 21st day, the wounds of animals from Group 2 (treated with CAH) were completely healed (Fig. 5-b4).

In vivo experiments showed that CAH can act as moist wound dressing due to its flexibility, permeability for water and metabolites, revealing its suitability for cleansing wounds by rehydrating dead tissues and enhancing autolytic debridement (Boateng et al., 2008; Kirschner & Anseth, 2013; Ribeiro et al., 2013).

3.5.1. Histological analysis

The histological analysis of skin samples collected from the wounded site of animals from Group 1 showed that an acute inflammatory process occurred immediately after burn induction, as demonstrated by the presence of polymorphonuclear neutrophils (Fig. 5-a1). Furthermore, after 21 days (Fig. 5-a4), different inflammatory cells (granulocytes, macrophages and neutrophils) were also present at the wound. New capillary vessels and fibroblasts cells, involved in the production of collagen type III and other proteins from the ECM, were also observed. Although, skin full structural integrity was not completely restored.

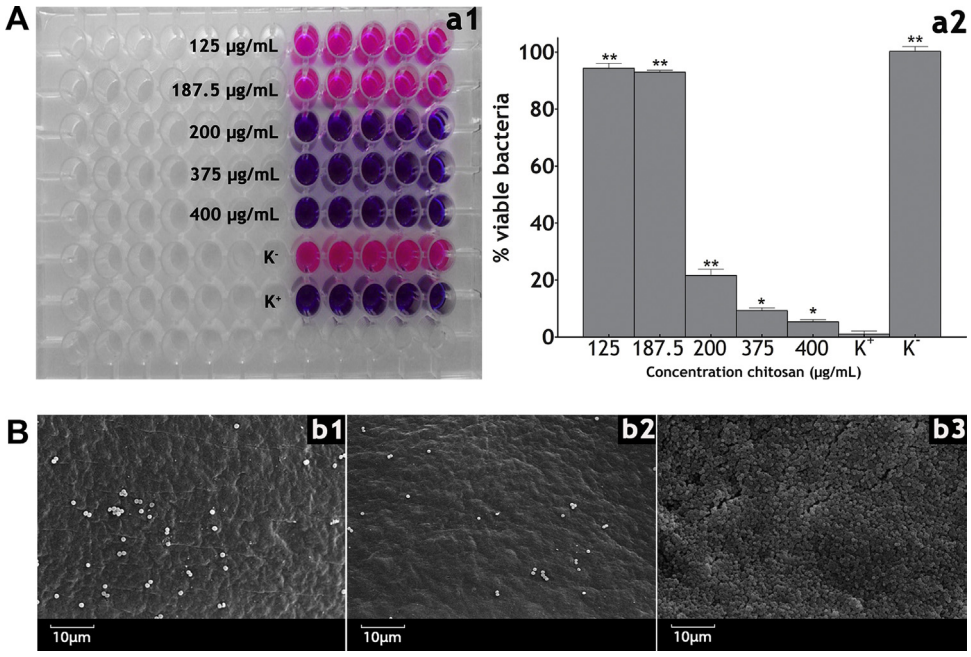

Fig. 4. Characterization of antibacterial properties of hydrogel: (A) Determination of MIC values through a Resazurin assay (a1). Blue color corresponds to the death bacteria and pink to the live bacteria. MIC values of the CAH after 24 h of incubation are presented in (a2). K^- (live bacteria); K^+ (death bacteria); agarose (ag); chitosan (Ch). Each result is the mean ± standart error of the mean of at least three independent experiments. Statistical analysis was performed using one-way ANOVA with Dunnet's post hoc test (* $p < 0.05$; ** $p < 0.01$); (B) SEM images of *Staphylococcus aureus* in contact with CAH produced with 200 μg/mL (b1) and 400 μg/mL (b2) of Ch. after 24 h. Negative control is presented in b3.

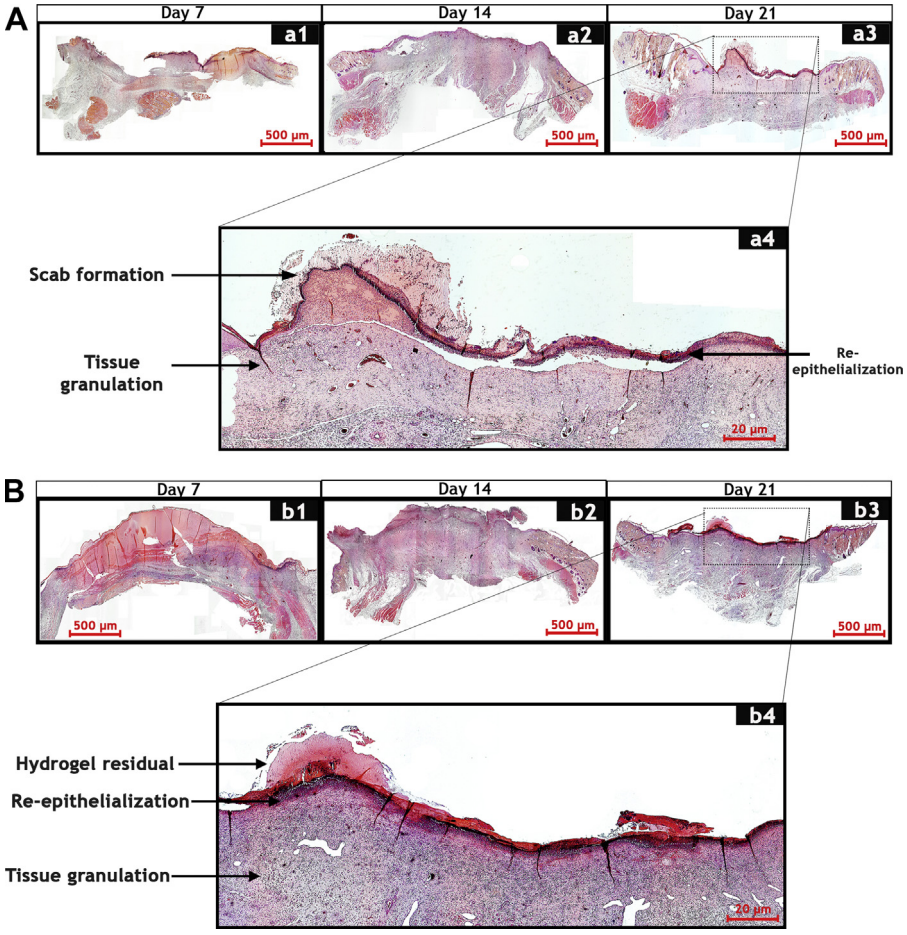

Fig. 5. Hematoxylin and eosin-stained sections of collected tissue samples for morphological evaluation of wounds after 7, 14 and 21 days. Group 1 treated with saline solution (A) and group 2 treated with CAH (3% ag–1.5% Ch). Agarose (ag); Chitosan (Ch).

Fig. 5B presents the panorama of the wound healing process that occurred in animals treated with CAH (group 2). These animals presented a re-epithelization of the wounds completely different from that of non-treated wounds. Seven days after injury was induced (Fig. 5-b1) no signs of acute inflammation were observed at the wound site.

Fibroblast cells were visible at the wound surface and granulation tissue was formed. On day 21 (Fig. 5-b4), the area of the granulation tissue is higher than that presented by animals from group 1. Moreover, dermis formation and re-epithelization (the thickness of epidermis increased) occurred in group 2 but not in the control group.

The results obtained clearly demonstrate that the agarose/chitosan based hydrogel improves the wound healing process, and avoids bacterial infection at the wound site (Berger et al., 2004). The thermoresponsive character of agarose is also fundamental to allow the gel to be applied directly at the desired site, without causing harmful side effects.

4. Conclusions

Based on all data collected, the produced hydrogel provides an adequate wound-healing environment that fulfils the required criteria set forth for an "ideal" wound dressing. Specifically, the wounds covered with CAH were moist and hydrated, demonstrating that water loss and wound dehydration was prevented. The high cellular proliferation at hydrogels surface suggests that nutrients, oxygen and carbon dioxide exchange occurred and accomplish all demands within wound. No signs of bacterial infection have been observed at the wound site, emphasizing that CAH bacterial properties can avoid delays or absence of healing.

In a near future, the addition of other ECM components or growth and differentiation factors to the CAH will further improve the wound repair.

Acknowledgments

The authors would like to thank Ana Paula Gomes for acquiring SEM images and Dr. Catarina Ferreira for her technical support in the preparation of histological samples. The authors would like to acknowledge the financial support provided by the Portuguese Foundation for Science and Technology (FCT) and (PEst-OE/EGE/UI4056/2011).

Appendix A. Supplementary data

Supplementary data associated with this article can be found, in the online version, at http://dx.doi.org/10.1016/j.carbpol.2014.04.093.

References

Atiyeh, B. S., & Hayek, S. N. (2005). State of the art in burn treatment. *World Journal of Surgery*, *29*(2), 131–148.

Aziz, M. A., Cabral, J. D., Brooks, H. J., Moratti, S. C., & Hanton, L. R. (2012). Antimicrobial properties of a chitosan dextran-based hydrogel for surgical use. *Antimicrobial Agents and Chemotherapy*, *56*(1), 280–287.

Balakrishnan, B., Mohanty, M., Umashankar, P., & Jayakrishnan, A. (2005). Evaluation of an in situ forming hydrogel wound dressing based on oxidized alginate and gelatin. *Biomaterials*, *26*(32), 6335–6342.

Berger, J., Reist, M., Mayer, J., Felt, O., Peppas, N., & Gurny, R. (2004). Structure and interactions in covalently and ionically crosslinked chitosan hydrogels for biomedical applications. *European Journal of Pharmaceutics and Biopharmaceutics*, *57*(1), 19–34.

Bhat, S., & Kumar, A. (2012). Cell proliferation on three-dimensional chitosan–agarose–gelatin cryogel scaffolds for tissue engineering applications. *Journal of Bioscience and Bioengineering*, *114*(6), 663–670.

Bhat, S., Tripathi, A., & Kumar, A. (2011). Supermacroprous chitosan–agarose–gelatin cryogels: In vitro characterization and in vivo assessment for cartilage tissue engineering. *Journal of The Royal Society Interface*, *8*(57), 540–554.

Boateng, J. S., Matthews, K. H., Stevens, H. N., & Eccleston, G. M. (2008). Wound healing dressings and drug delivery systems: A review. *Journal of Pharmaceutical Sciences*, *97*(8), 2892–2923.

Böttcher-Haberzeth, S., Biedermann, T., & Reichmann, E. (2010). Tissue engineering of skin. *Burns*, *36*(4), 450–460.

Buckley, C. T., Thorpe, S. D., O'Brien, F. J., Robinson, A. J., & Kelly, D. J. (2009). The effect of concentration, thermal history and cell seeding density on the initial mechanical properties of agarose hydrogels. *Journal of the Mechanical Behavior of Biomedical Materials*, *2*(5), 512–521.

Busilacchi, A., Gigante, A., Mattioli-Belmonte, M., Manzotti, S., & Muzzarelli, R. A. (2013). Chitosan stabilizes platelet growth factors and modulates stem cell differentiation toward tissue regeneration. *Carbohydrate Polymers*, *98*(1), 665–676.

Cao, Z., Gilbert, R. J., & He, W. (2009). Simple agarose–chitosan gel composite system for enhanced neuronal growth in three dimensions. *Biomacromolecules*, *10*(10), 2954–2959.

Correia, T. R., Antunes, B. P., Castilho, P. H., Nunes, J. C., Pessoa de Amorim, M. T., Escobar, I. C., Queiroz, J. A., Correia, I. J., & Morão, A. M. (2013). A bi-layer electrospun nanofiber membrane for plasmid DNA recovery from fermentation broths. *Separation and Purification Technology*, *112*, 20–25.

Evers, L. H., Bhavsar, D., & Mailänder, P. (2010). The biology of burn injury. *Experimental Dermatology*, *19*(9), 777–783.

Faucheux, N., Schweiss, R., Lützow, K., Werner, C., & Groth, T. (2004). Self-assembled monolayers with different terminating groups as model substrates for cell adhesion studies. *Biomaterials*, *25*(14), 2721–2730.

Fedtke, I., Götz, F., & Peschel, A. (2004). Bacterial evasion of innate host defenses—The *Staphylococcus aureus* lesson. *International Journal of Medical Microbiology*, *294*(2), 189–194.

Felt, O., Carrel, A., Baehni, P., Buri, P., & Gurny, R. (2000). Chitosan as tear substitute: A wetting agent endowed with antimicrobial efficacy. *Journal of Ocular Pharmacology and Therapeutics*, *16*(3), 261–270.

Francis Suh, J. K., & Matthew, H. W. T. (2000). Application of chitosan-based polysaccharide biomaterials in cartilage tissue engineering: A review. *Biomaterials*, *21*(24), 2589–2598.

Gaspar, V., Sousa, F., Queiroz, J., & Correia, I. (2010). Formulation of chitosan–TPP–pDNA nanocapsules for gene therapy applications. *Nanotechnology*, *22*(1), 015101.

Gaspar, V. M., Correia, I. J., Sousa, Â., Silva, F., Paquete, C. M., Queiroz, J. A., & Sousa, F. (2011). Nanoparticle mediated delivery of pure P53 supercoiled plasmid DNA for gene therapy. *Journal of Controlled Release*, *156*(2), 212–222.

Gonzalez, R., & Tarloff, J. (2001). Evaluation of hepatic subcellular fractions for Alamar blue and MTT reductase activity. *Toxicology In Vitro*, *15*(3), 257–259.

Hersel, U., Dahmen, C., & Kessler, H. (2003). RGD modified polymers: Biomaterials for stimulated cell adhesion and beyond. *Biomaterials*, *24*(24), 4385–4415.

Hirano, S., & Noishiki, Y. (2004). The blood compatibility of chitosan and *N*-acylchitosans. *Journal of Biomedical Materials Research*, *19*(4), 413–417.

Hutmacher, D., Goh, J., & Teoh, S. (2001). An introduction to biodegradable materials for tissue engineering applications. *Annals of the Academy of Medicine (Singapore)*, *30*(2), 183

Jayakumar, R., Prabaharan, M., Sudheesh Kumar, P., Nair, S., & Tamura, H. (2011). Biomaterials based on chitin and chitosan in wound dressing applications. *Biotechnology Advances*, *29*(3), 322–337.

Jeong, B., Kim, S. W., & Bae, Y. H. (2012). Thermosensitive sol–gel reversible hydrogels. *Advanced Drug Delivery Reviews*, *54*(1), 37–51.

Juan, L., Zhimin, Z., Anchun, M., Lei, L., & Jingchao, Z. (2010). Deposition of silver nanoparticles on titanium surface for antibacterial effect. *International Journal of Nanomedicine*, *5*, 261–267.

Kathuria, N., Tripathi, A., Kar, K. K., & Kumar, A. (2009). Synthesis and characterization of elastic and macroporous chitosan–gelatin cryogels for tissue engineering. *Acta Biomaterialia*, *5*(1), 406–418.

Kim, I. Y., Seo, S. J., Moon, H. S., Yoo, M. K., Park, I. Y., Kim, B. C., & Cho, C. S. (2008). Chitosan and its derivatives for tissue engineering applications. *Biotechnology Advances*, *26*(1), 1–21.

Kirschner, C. M., & Anseth, K. S. (2013). Hydrogels in healthcare: From static to dynamic material microenvironments. *Acta Materialia*, *61*(3), 931–944.

Lakes, R. S. (2007). *Biomaterials: an introduction* (3rd ed.). USA: Springer.

Lee, D. W., Lim, H., Chong, H. N., & Shim, W. S. (2009). Advances in chitosan material and its hybrid derivatives: A review. *Open Biomaterials Journal*, *1*, 10–20.

Li, Z., Ramay, H. R., Hauch, K. D., Xiao, D., & Zhang, M. (2005). Chitosan–alginate hybrid scaffolds for bone tissue engineering. *Biomaterials*, *26*(18), 3919–3928.

Lima, A. C., Batista, P., Valente, T. A., Silva, A. S., Correia, I. J., & Mano, J. F. (2013). Novel methodology based on biomimetic superhydrophobic substrates to immobilize cells and proteins in hydrogel spheres for applications in bone regeneration. *Tissue Engineering A*, *19*(9–10), 1175–1187.

Mano, J., Silva, G., Azevedo, H. S., Malafaya, P., Sousa, R., Silva, S., Boesel, L., Oliveira, J. M., Santos, T., & Marques, A. (2007). Natural origin biodegradable systems in tissue engineering and regenerative medicine: Present status and some moving trends. *Journal of The Royal Society Interface*, *4*(17), 999–1030.

Marques, J. G., Gaspar, V. M., Costa, E., Paquete, C. M., & Correia, I. J. (2014). Synthesis and characterization of micelles as carriers of non-steroidal anti-inflammatory drugs (NSAID) for application in breast cancer therapy. *Colloids and Surfaces B: Biointerfaces*, *113*, 375–383.

Martin, B. C., Minner, E. J., Wiseman, S. L., Klank, R. L., & Gilbert, R. J. (2008). Hydrogel blends for support of nerve regeneration therapies. *Journal of Neural Engineering*, *5*, 221–231.

Medina-Esquivel, R., Freile-Pelegrin, Y., Quintana-Owen, P., Yáñez-Limón, J., & Alvarado-Gil, J. (2008). Measurement of the sol–gel transition temperature in agar. *International Journal of Thermophysics*, *29*(6), 2036–2045.

Metcalfe, A. D., & Ferguson, M. (2007). Bioengineering skin using mechanisms of regeneration and repair. *Biomaterials*, *28*(34), 5100.

Mi, F. L., Wu, Y. B., Shyu, S. S., Schoung, J. Y., Huang, Y. B., Tsai, Y. H., & Hao, J. Y. (2002). Control of wound infections using a bilayer chitosan wound dressing with sustainable antibiotic delivery. *Journal of Biomedical Materials Research*, *59*(3), 438–449.

Muzzarelli, R. A. A. (1997). Human enzymatic activities related to the therapeutic administration of chitin derivatives. *Cellular and Molecular Life Sciences*, *53*(2), 131–140.

Muzzarelli, R. A. A. (2009). Chitins and chitosans for the repair of wounded skin, nerve, cartilage and bone. *Carbohydrate Polymers*, *76*(2), 167–182.

Muzzarelli, R. A. A., & Rocchetti, R. (1985). Determination of the degree of acetylation of chitosans by first derivative ultraviolet spectrophotometry. *Carbohydrate Polymers*, *5*(6), 461–472.

Nicodemus, G. D., & Bryant, S. J. (2008). Cell encapsulation in biodegradable hydrogels for tissue engineering applications. *Tissue Engineering B*, *14*(2), 149–165.

Oliveira, S. M., Alves, N. M., & Mano, J. F. (2012). Cell interactions with superhydrophilic and superhydrophobic surfaces. *Journal of Adhesion Science and Technology*, *27*(24), 1–21.

Palmeira-de-Oliveira, A., Ribeiro, M., Palmeira-de-Oliveira, R., Gaspar, C., Costa-de-Oliveira, S., Correia, I., Pina Vaz, C., Martinez-de-Oliveira, J., Queiroz, J., & Rodrigues, A. (2010). Anti-candida activity of a chitosan hydrogel: Mechanism of action and cytotoxicity profile. *Gynecologic and Obstetric Investigation*, *70*(4), 322–327.

Pasparakis, G., & Bouropoulos, N. (2006). Swelling studies and in vitro release of verapamil from calcium alginate and calcium alginate–chitosan beads. *International Journal of Pharmaceutics*, *323*(1), 34–42.

Paul, W., & Sharma, C. P. (2004). Chitosan and alginate wound dressings: A short review. *Trends in Biomaterials and Artificial Organs*, *18*(1), 18–23.

Reinke, J., & Sorg, H. (2012). Wound repair and regeneration. *European Surgical Research*, *49*(1), 35–43.

Ribeiro, M., Morgado, P., Miguel, S., Coutinho, P., & Correia, I. (2013). Dextran based-hydrogel containing chitosan microparticles loaded with growth factors to be used in wound healing. *Materials Science and Engineering: C*, *33*(5), 2958–2966.

Ribeiro, M. P., Espiga, A., Silva, D., Baptista, P., Henriques, J., Ferreira, C., Silva, J. C., Borges, J. P., Pires, E., & Chaves, P. (2009). Development of a new chitosan hydrogel for wound dressing. *Wound Repair and Regeneration*, *17*(6), 817–824.

Schuetz, Y. B., Gurny, R., & Jordan, O. (2008). A novel thermoresponsive hydrogel based on chitosan. *European Journal of Pharmaceutics and Biopharmaceutics*, *68*(1), 19–25.

Silva, S., Moreira-Silva, J., Silva, T. H., Perez-Martin, R. I., Sotelo, C. G., Mano, J. F., Duarte, A. R. C., & Reis, R. L. (2013). Porous hydrogels from shark skin collagen crosslinked under dense carbon dioxide atmosphere. *Macromolecular Bioscience*, *13*(11), 1621–1631.

Trivedi, T. J., Rao, K. S., & Kumar, A. (2014). Facile preparation of agarose–chitosan hybrid materials and nanocomposite ionogels using an ionic liquid via dissolution, regeneration and sol–gel transition. *Green Chemistry*, *16*(1), 320–330.

Valente, J., Gaspar, V., Antunes, B., Countinho, P., & Correia, I. (2012). Microencapsulated chitosan–dextran sulfate nanoparticles for controled delivery of bioactive molecules and cells in bone regeneration. *Polymer*, *54*(1), 5–15.

van der Flier, A., & Sonnenberg, A. (2001). Function and interactions of integrins. *Cell and Tissue Research*, *305*(3), 285–298.

Varoni, E., Tschon, M., Palazzo, B., Nitti, P., Martini, L., & Rimondini, L. (2012). Agarose gel as biomaterial or scaffold for implantation surgery: Characterization, histological and histomorphometric study on soft tissue response. *Connective Tissue Research*, *53*(6), 548–554.

Weng, L., Romanov, A., Rooney, J., & Chen, W. (2008). Non-cytotoxic, in situ gelable hydrogels composed of *N*-carboxyethyl chitosan and oxidized dextran. *Biomaterials*, *29*(29), 3905–3913.

Winter, G. D. (1974). Transcutaneous implants: Reactions of the skin-implant interface. *Journal of Biomedical Materials Research*, *8*(3), 99–113.

Xu, X. L., Lou, J., Tang, T., Ng, K. W., Zhang, J., Yu, C., & Dai, K. (2005). Evaluation of different scaffolds for BMP-2 genetic orthopedic tissue engineering. *Journal of Biomedical Materials Research B: Applied Biomaterials*, *75*(2), 289–303.

Yu, L., & Ding, J. (2008). Injectable hydrogels as unique biomedical materials. *Chemical Society Reviews*, *37*(8), 1473–1481.

Zhang, L., Guo, J., Peng, X., & Jin, Y. (2004). Preparation and release behavior of carboxymethylated chitosan/alginate microspheres encapsulating bovine serum albumin. *Journal of Applied Polymer Science*, *92*(2), 878–882.